Talanta 135 (2015) 34–40

Contents lists available at ScienceDirect

Talanta

journal homepage: www.elsevier.com/locate/talanta

Screen-printed electrode based electrochemical detector coupled with ionic liquid dispersive liquid–liquid microextraction and microvolume back-extraction for determination of mercury in water samples

Elena Fernández [a], Lorena Vidal [a,*], Daniel Martín-Yerga [b], María del Carmen Blanco [b], Antonio Canals [a,*], Agustín Costa-García [b]

[a] Departamento de Química Analítica, Nutrición y Bromatología e Instituto Universitario de Materiales, Universidad de Alicante, P.O. Box 99, E-03080 Alicante, Spain

[b] Departamento de Química Física y Analítica, Universidad de Oviedo, C/Julián Clavería, 8, 33006 Oviedo, Spain

ARTICLE INFO

Article history:
Received 31 July 2014
Received in revised form
31 October 2014
Accepted 4 November 2014
Available online 18 December 2014

Keywords:
Liquid-phase microextraction
Dispersive liquid–liquid microextraction
Ionic liquid
Mercury
Screen-printed electrode
Water samples

ABSTRACT

A novel approach is presented, whereby gold nanostructured screen-printed carbon electrodes (SPCnAuEs) are combined with in-situ ionic liquid formation dispersive liquid–liquid microextraction (in-situ IL-DLLME) and microvolume back-extraction for the determination of mercury in water samples. In-situ IL-DLLME is based on a simple metathesis reaction between a water-miscible IL and a salt to form a water-immiscible IL into sample solution. Mercury complex with ammonium pyrrolidinedithiocarbamate is extracted from sample solution into the water-immiscible IL formed in-situ. Then, an ultrasound-assisted procedure is employed to back-extract the mercury into 10 μL of a 4 M HCl aqueous solution, which is finally analyzed using SPCnAuEs.

Sample preparation methodology was optimized using a multivariate optimization strategy. Under optimized conditions, a linear range between 0.5 and 10 $\mu g\,L^{-1}$ was obtained with a correlation coefficient of 0.997 for six calibration points. The limit of detection obtained was 0.2 $\mu g\,L^{-1}$, which is lower than the threshold value established by the Environmental Protection Agency and European Union (i.e., 2 $\mu g\,L^{-1}$ and 1 $\mu g\,L^{-1}$, respectively). The repeatability of the proposed method was evaluated at two different spiking levels (3 and 10 $\mu g\,L^{-1}$) and a coefficient of variation of 13% was obtained in both cases. The performance of the proposed methodology was evaluated in real-world water samples including tap water, bottled water, river water and industrial wastewater. Relative recoveries between 95% and 108% were obtained.

1. Introduction

Mercury is one of the most well-known toxic elements and even the World Health Organization places it between the first ten chemicals or group of chemicals of major public health concern [1]. Mercury exists in different forms with different properties, namely elemental or metallic (i.e., Hg^0); inorganic (i.e., Hg^{2+}); and organic (i.e., $MeHg^+$, $EtHg^+$, $PhHg^+$). Several factors determine the adverse effects from mercury exposure including its chemical form, the dose, the age and health of the person exposed, and the duration and kind of exposure (e.g., inhalation, ingestion, etc.) [2]. Among the most relevant health effects we can mention damage to the gastrointestinal tract, nervous system, kidneys, respiratory failures and problems during the development of organs in unborn.

Mercury enters in the environment through both biogenic and anthropogenic vias. However, human activities such as mining, burning of fossil fuels, agriculture, paper and electrochemical industries, and household wastes, are the main responsible of the concerning increase of mercury levels in air, soil and water of certain contaminated areas. Monitoring the presence of mercury in natural and drinking waters is of great interest due to its high toxicity and bioaccumulation factor [3]. Mercury concentrations are commonly in the range of low $ng\,L^{-1}$ in environmental waters [3] whereas the permitted level of mercury in drinking water depends on the responsible authorities of each territory. For example, the Environmental Protection Agency (EPA) sets the threshold level at 2 $\mu g\,L^{-1}$ [4], but the European Union establishes the limit at 1 $\mu g\,L^{-1}$ [5].

* Corresponding authors. Tel./fax: +34 965909790.
E-mail addresses: lorena.vidal@ua.es (L. Vidal), a.canals@ua.es (A. Canals).

http://dx.doi.org/10.1016/j.talanta.2014.11.069
0039-9140/

Electrochemical techniques have been widely employed to determine mercury in natural and drinking waters. Two excellent reviews have been recently published about the latest advances in electrochemical, mainly voltammetric, determination of mercury [6,7]. Electrochemistry offers sensitivity, simplicity, rapid response and inexpensive instrumentation with miniaturization and portable options. A major drawback to be considered results from the difficulty of removing mercury from electrode surface between measurements which leads to memory effect problems [6,7]. However, tedious and time consuming cleaning steps can be avoided with the use of screen-printed electrodes (SPEs), which can be disposable after a single use due to their high cost effectiveness. Several methods based on SPEs have been reported for the determination of mercury in different water samples, including the use of bare gold SPEs [8], and modified SPEs with carbon nanomaterials [9–11], gold films [12,13], gold nanoparticles [14,15], nanohybrid materials [14] and chelating agents [16]. As can be seen in Table 1, the vast majority of the reported works include a preconcentration step over the working electrode (i.e., deposition time) followed by anodic stripping voltammetry. Gold is commonly employed in working electrodes due to its high affinity for mercury which leads to an improvement in its preconcentration. In addition, mercury suffers from a process named underpotential deposition (UPD) on gold electrodes [7]. The presence of gold promotes the adsorption of mercury atoms on the surface once the ionic metal is reduced forming an amalgam (Au–Hg). The formation of this amalgam is energetically more favored with respect to pure mercury and makes the deposition of mercury on gold occur at a more positive potential than in normal conditions. As a consequence, the selectivity of the method is generally improved. In this work, screen-printed carbon electrodes modified with gold nanoparticles (SPCnAuEs) are employed as electrochemical transducers in the detection stage. The use of nanoparticles in electroanalysis is continuously growing due to its numerous advantages, related to the unique properties of nanoparticulate materials [17] (e.g., increasing surface area, enhanced mass transport and improving selectivity, catalytic activity and signal to noise ratio).

Liquid-phase microextraction (LPME) [18] appeared in the latest nineties offering undoubted advantages as miniaturized extraction techniques, such as simplicity, easiness to handle, low sample and solvent consumptions, and an important reduction of residues generated. One of the most popular LPME technique is dispersive liquid–liquid microextraction (DLLME) [19] which has even come to dominate LPME research publications in the recent years [20]. DLLME is based on the complete dispersion of the small volume of extractant solvent into the sample, normally assisted by a disperser agent. During DLLME, there is a high contact between phases therefore the extraction is really rapid and effective. After the extraction, phases are separated normally by centrifugation and the enriched phase with analyte is analyzed. Numerous modifications of the original DLLME procedure [19] have been reported up to now [21] including the use of new extractant solvents such as ionic liquids (ILs) [22]. Within the use of ILs, a novel methodology called in-situ IL formation dispersive liquid–liquid microextraction (in-situ IL-DLLME) [23,24] has recently been developed. In-situ IL-DLLME is based on the formation of a water-immiscible IL using a metathesis reaction between a water-miscible IL and an ion exchange salt into sample solution. Thereby, the extractant phase is generated in-situ in form of homogeneously dispersed fine drops, the disperser agent is totally avoided and the extraction efficiency generally increases.

Different LPME techniques including single-drop microextraction [25,26], DLLME [27–29], in-situ IL-DLLME [23] and task-specific IL ultrasound-assisted DLLME [30] have been employed for the determination and speciation of mercury in water samples. In these works, bulky and expensive chromatographic systems [25,28,29], capillary electrophoresis [27], UV–vis spectrometry [23], cold vapor [30] and electrothermal vaporization atomic absorption spectrometry [26] were used as separation and detection techniques, respectively.

The approach presented here employs an in-situ IL-DLLME followed by an ultrasound-assisted microvolume back-extraction and SPCnAuEs as electrochemical transducers for the determination of mercury in water samples. This combination exploits the advantages of including a miniaturized sample preparation step with the high sensitivity and specificity that offers the electrochemical determination of mercury using SPCnAuEs. LPME provides a high preconcentration of the analyte and a clean-up step for dirty matrices employing low amounts of sample and chemicals. In addition, considering the low volume of sample needed for analysis with SPEs, they appear as an alternative and perfectly compatible detection methodology after miniaturized extraction techniques, thus avoiding classical and bulky analytical instrumentation [31]. A multivariate optimization strategy has been adopted for the optimization of the sample preparation and the applicability of the method has been tested studying real-world water samples.

Table 1
Comparison of different methods using SPEs for the determination of mercury in water samples.

Electrode	Lineal range	LOD	Real water samples	Comments/analytical technique (deposition time in parentheses)	Ref.
SPGE	5–30 ng mL^{-1}	1.1 ng mL^{-1}	Wastewater and rain water	SWASV (60 s)	[8]
SPE/carbon black	2.5×10^{-8}–1×10^{-7} M (5–20 μg L^{-1})	5×10^{-9} M (1 μg L^{-1})	Drinking water	Indirect determination by amperometric measurements of thiols	[9]
SPBE/MWCNTs	0.2–40 μg L^{-1}	0.09 μg L^{-1}	Tap water	SWASV (180 s)	[10]
Carbon NPs-based SPEs	1–10 μg L^{-1}	–	Seawater	Heated electrodes/SWASV (120 s)	[11]
SPE/gold film	2–16 μg L^{-1}	1.5 μg L^{-1}	Tap water	SWASV (120 s)	[12]
SPE/gold film	0.2–0.8 μg L^{-1}	0.08 μg L^{-1}	–	Preconcentration step using magnetic nanoparticles modified with thiols/SWASV (120 s)	[12]
SPCE/gold film	0–100 μg L^{-1}	0.9 μg L^{-1}	–	SWASV (120 s)	[13]
SPGOnAuEs	2–50 μg L^{-1}	1.9 μg L^{-1}	–	SWASV (200 s)	[14]
SPCNTnAuEs	0.5–50 μg L^{-1}	0.2 μg L^{-1}	Tap and river waters	SWASV (200 s)	[14]
SPCnAuEs	5–100 μg L^{-1}	3.3 μg L^{-1}	–	SWASV (240 s)	[14]
SPCnAuEs	5–20 ng mL^{-1}	0.8 ng mL^{-1}	Rain and river waters, industrial wastewater	SWASV (120 s)	[15]
CTS-SPE	20–80 ng mL^{-1}	2 ng mL^{-1}	–	DPASV (30 s)	[16]

SPGE, screen-printed gold electrode; SWASV, square-wave anodic stripping voltammetry; SPBE, screen-printed bismuth electrode; MWCNTs, multi-walled carbon nanotubes; NPs, nanoparticles; SPGOnAuEs, screen-printed graphene oxide/gold nanoparticles electrodes; SPCNTnAuEs, screen-printed carbon nanotubes/gold nanoparticles electrodes; DPASV, differential-pulse anodic stripping voltammetry; CTS-SPE, chitosan-modified screen-printed electrodes.

2. Experimental part

2.1. Reagents and water samples

A stock standard solution of Hg^{2+} (1000 mg L^{-1}) was prepared by dissolving $Hg(OAc)_2$ (≥ 99%) from Fluka (Stenhein, Germany) in ultrapure water. Working solutions were prepared by proper dilution of the stock standard. The 1-hexyl-3-methylimidazolium chloride IL ([Hmim][Cl]) (98%) was purchased from Iolitec (Heilbronn, Germany). The lithium bis[(trifluoromethyl)sulfonyl]imide ($LiNTf_2$) salt and the chelating agent ammonium pyrrolidinedithiocarbamate (APDC) (~99%) were supplied by Sigma-Aldrich (St. Louis, MO, USA). A solution of 2 mg mL^{-1} of the chelating agent was prepared by dissolving APDC in ultrapure water. Reactive grade NaCl and NaOH (≥ 97%, pellets) were from ACS Scharlau (Barcelona, Spain). Fuming HCl (37%) was supplied by Merck (Madrid, Spain). The ultrapure water employed for preparing all solutions was obtained with a Millipore Direct System Q5™ purification system from Ibérica S.A. (Madrid, Spain).

Standard Au^{3+} tetrachloro complex (1.000 ± 0.002 g of $AuCl_4^-$ in 500 mL of 1.0 M HCl) was purchased from Merck. Solutions of 1 mM $AuCl_4^-$ were prepared by suitable dilution of this standard solution in 0.1 M HCl.

Tap water was collected from the water-supplied network of the lab in the Departament of Physical and Analytical Chemistry of the University of Oviedo (Spain). Bottled water (San Benedetto mineral water, Valencia, Spain) was purchased in the supermarket. River water from Nora river was collected in Tiñana (Siero, Spain) and industrial wastewater was from Galicia (Spain). The wastewater contained a chemical oxygen demand of 7 mg O_2 L^{-1} and $< \cdot 5$ mg L^{-1} of suspended solids. All water samples were stored at 4 °C and were used without any further pretreatment. Initial analysis with the developed method confirmed that mercury levels were undetectable in the four selected water samples.

2.2. Apparatus and electrodes

An ultrasounds bath from Elma (Singen, Germany) was used to assist the back-extraction procedure.

An Autolab PGSTAT 12 potentiostat from EcoChemie (Ultrecht, The Netherlands) controlled by Autolab GPES software version 4.8 was used for electrochemical experiments.

Screen-printed carbon electrodes (SPCEs) (ref. DRP-110) with three electrode configuration were purchased from DropSens (Oviedo, Spain). The working electrode, with a disk-shaped of 4 mm of diameter, and the counter electrode were made of a carbon ink whereas the pseudo-reference electrode was made of silver. Specific connectors obtained from DropSens (ref. DRP-DSC) were used for the conexion of the SPCEs to the potentiostat.

2.3. In-situ IL-DLLME and microvolume back-extraction

Under optimum conditions, 20 mg of [Hmim][Cl] were placed in a test tube and dissolved in 4 mL of aqueous standards or sample solutions and the chelating agent (40 μL of 2 mg mL^{-1}). The ionic exchange salt $LiNTf_2$ was added in an equimolar ratio (i.e., 28.3 mg) with the IL [Hmim][Cl], according to previous works [24,31]. A cloudy solution was immediately formed and the mixture was manually shaken for 0.5 min. In order to accelerate phases separation, the tube was then introduced in an ice bath for 5 min. Next, the phases were separated by centrifugation for 10 min at 5000 rpm. The aqueous phase was removed with a glass pipette, and the formed IL-phase (i.e., 20 μL of [Hmim][NTf_2]) was withdrawn with a micropipette and deposited in an Eppendorf tube of 0.5 mL. For the back-extraction, 10 μL of 4 M HCl aqueous solution was added to the IL phase and the mixture was sonicated in an ultrasounds bath for 14 min at 90% of power and 37 KHz of frequency. Since direct measurements on the IL were not suitable, back-extraction was necessary for voltammetric analysis. After back-extraction, phases were separated by centrifugation for 5 min at 5000 rpm and the enriched acidic aqueous phase that remained in the upper part was analyzed. The overall procedure is graphically described in Fig. 1.

2.4. Electrochemical analysis

Gold nanoparticles were generated over the SPCEs surface employing the procedure developed by Martínez-Paredes et al. [32] and previously optimized by Martín-Yerga et al. for the determination of mercury [14]. Briefly, 40 μL of a 1 mM $AuCl_4^-$ solution in 0.1 M HCl aqueous solution were dropped onto the SPCE surface and a constant current of −100 μA was applied for 180 s. After gold nanoparticles deposition, the electrode surface was generously rinsed with ultrapure water and dried at room temperature before use. A new SPCnAuEs was prepared and employed for each experiment. The electrochemical behavior of mercury on SPCnAuEs was previously and deeply studied [14], therefore, no further discussion will be included in the present work.

After back-extraction, 5 μL of the resulting upper acidic aqueous phase was mixed with 37 μL of 0.5 M NaOH in order to obtain a suitable electrolytic medium. A volume of 40 μL of this solution was deposited on the electrode surface for voltammetric measurements. Mercury was determined by square-wave anodic stripping voltammetry employing previous optimized conditions [14]. Mercury was preconcentrated over SPCnAuEs by applying a constant potential of +0.3 V for 240 s. Thereafter, the potential was recorded between +0.3 V and +0.55 V at a frequency of 80 Hz, amplitude of 30 mV and step potential of 4 mV. All experiments were carried out at room temperature.

2.5. Data processing

An anodic peak corresponding to the reoxidation of mercury appears at approximately +0.42 V and the height of this peak was employed for the quantification of the analyte. The “base line correction” option provided by GPEs software was employed to get more defined peaks, specially at low concentrations, and to obtain more reliable and accurate measurements.

A two-step multivariate optimization strategy, using Plackett–Burman and central composite designs, was carried out to determine the optimum conditions of sample preparation. Minitab 15 statistical software (State College, PA, USA) was employed to construct the experimental design matrices and evaluate the results.

3. Results and discussion

3.1. Optimization of sample preparation

3.1.1. Screening step

Plackett–Burman design is a two-level fractional factorial design that ignores interaction between factors and therefore main effects can be calculated with a reduced number of experiments leading to a saving in resources and time. The Plackett–Burman design results are very useful in the first steps of a project when many factors are initially considered but finally only a few show important effects [33]. A saturated Plackett–Burman design was used to construct the matrix of experiments, including 11 factors: eight real factors and three dummy factors. The effects of dummy factors were used to evaluate the experimental error [34,35]. The eight real experimental factors selected at two levels were: amount of [Hmim][Cl], amount of chelating agent, ionic strength, sample pH, volume of HCl acceptor solution during back-extraction, back-extraction time, power and

frequency of the ultrasounds bath. Table 2 shows the experimental factors and levels considered in the Plackett–Burman design. A total of twelve experiments were randomly performed using aqueous standards of 25 μg L^{-1}.

The data obtained were evaluated using an ANOVA test and the results were visualized with the Pareto chart shown in Fig. S1 (Supplementary material). The length of each bar was proportional to the influence of the corresponding factor and the effects that exceed each reference vertical line can be considered significant with 95% and 90% probability, respectively.

According to Fig. S1, the ultrasounds frequency and HCl volume were statistically significant factors, with 95% probability, showing a negative effect. The negative effect of the frequency is in agreement with the fact that at high ultrasounds frequencies, cavitation bubbles are more difficult to create as a result of the shorter duration of rarefraction cycles. Higher amplitudes (i.e., power) would be necessary to ensure that cohesive forces in the liquid were overcome and maintain a certain cavitational energy [36]. For the HCl volume, the negative effect is easily explained considering that if less volume of acid is used, a higher concentration of the analyte is obtained in the final acceptor solution. The ultrasounds device employed during this work only accepted two discrete values of frequency, namely 37 and 80 KHz, thus this significant factor could not be included in the following optimization step and was fixed in its lower level. As a consequence, back-extraction time and amount of [Hmim][Cl], which showed significant effects with 90% probability (see Fig. S1), were included in the next optimization step. Back-extraction time showed a positive effect whereas for the amount of [Hmim][Cl] the effect was negative. These effects revealed that the mass transfer during back-extraction is not as instantaneous as during in-situ IL-DLLME, and it is enhanced if low amounts of [Hmim][NTf_2] are formed, probably related to diffusion effects from the bulk of the IL to the contact surface with the HCl aqueous solution.

The other four real factors considered in screening step with non-significant effects were fixed at the following levels: amount of chelating agent, 40 μL (2 mg mL^{-1}); ionic strength, no addition of NaCl; sample pH, the pH of water without any adjustment; and ultrasounds power, 90%.

3.1.2. *Optimization of significant factors*

Central composite design (CCD) combines a two-level full factorial design (2^k) with $2k$ star points, where k is the number of factors being optimized, and one point at the center of the experimental region. In order to ensure the rotatability of the model, star points were set at $\alpha = \sqrt[4]{2^k} = 1.682$ whereas the central point was repeated five times to provide an orthogonal design [33]. CCD was used to evaluate and optimize main effects, interaction effects and quadratic effects of the three considered factors. Table 3 shows the low and high levels, the central and star points of the considered factors in the optimization step. Nineteen experiments were randomly performed using aqueous standards of 25 μg L^{-1}.

Table 2
Experimental factors and levels of the Plackettt–Burman design.

Factors	Level	
	Low (−1)	High (+1)
Amount of [Hmim][Cl] (mg)	20	40
Amount of chelating agent (μL, 2 mg mL^{-1})	20	40
Ionic strength (NaCl concentration, %, w/v)	0	10
Sample pH	5	10
HCl volume (μL)	20	50
Back-extraction time (min)	5	10
Ultrasounds power (%)	50	90
Ultrasounds frequency (KHz)	37	80

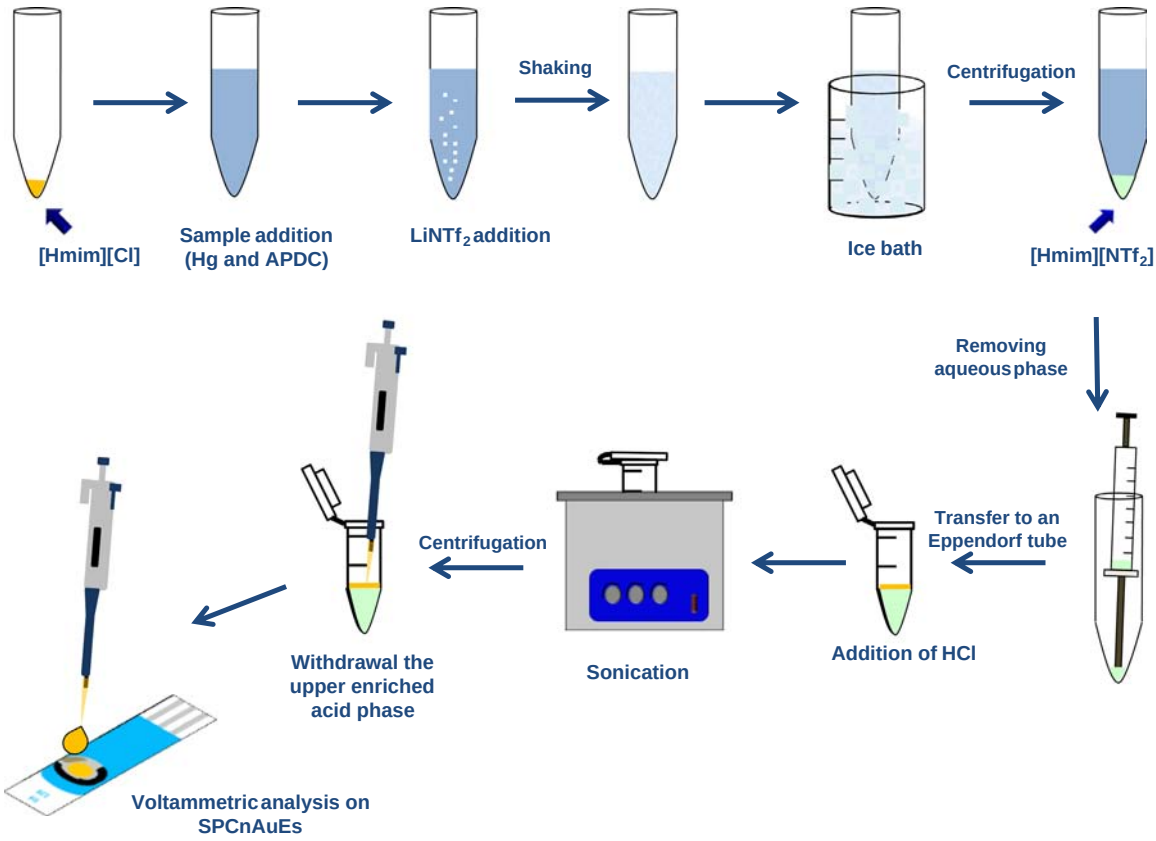

Fig. 1. In-situ IL-DLLME and ultrasound-assisted microvolume back-extraction coupled with SPCnAuE.

Table 3
Factors, low and high levels, central and star points used in CCD design.

Factor	Level			Star points (α=1.682)	
	Low (−1)	Central (0)	High (+1)	$-\alpha$	$+\alpha$
HCl volume (μL)	22	40	58	10	70
Back-extraction time (min)	6	10	14	3	17
Amount of [Hmim][Cl] (mg)	28	40	52	20	60

The data obtained were also evaluated using an ANOVA test. The coefficients of the factors and the *p*-values are listed in Table S1 (Supplementary material).

Significant factors with 95% probability (i.e., p-value < 0.05) were HCl volume, back-extraction time and the quadratic effects of back-extraction time and amount of [Hmim][Cl], which confirms the curvature of the system and its fitting with the proposed second-grade polynomial system. The adjustment obtained expressed as r^2 value was 92%.

The response surfaces obtained using the CCD are shown in Fig. 2. Pairs of factors were considered separately in order to easily interpret the effect of each one on the response of the system. Thus, Fig. 2a shows the response surface which results in plotting HCl volume vs. back-extraction time, for 40 mg of [Hmim][Cl]; Fig. 2b shows the response surface obtained as a function of HCl volume and amount of [Hmim][Cl], whilst back-extraction time is fixed at 10 min; and Fig. 2c shows the surface response corresponding the effects of back-extraction time and amount of [Hmim][Cl], with established HCl volume at 40 μL. As expected, HCl volume has a negative effect (Fig. 2a and b) and the response of the system increases when the HCl volume decreases. For the back-extraction time, the response of the system increases with the time (Fig. 2a and c) until reaching a maximum at 14 min. Both, 10 μL for HCl volume and 14 min for the back-extraction time, were adopted as the optimum conditions for the proposed methodology. As can be seen in Fig. 2b and c, the effect of the amount of [Hmim][Cl] also presents a maximum over 40 mg, although the variation of the response is really slight between 40 and 20 mg. Thus, considering the sign of the effect of this factor obtained in the Plackett–Burman design, which was negative, and the importance of waste reduction, 20 mg of [Hmim][Cl] were finally chosen for the validation of the method.

In summary, the results obtained from the overall optimization process lead to the following experimental conditions: amount of [Hmim][Cl], 20 mg; amount of chelating agent, 40 μL (2 mg mL^{-1}); ionic strength, no addition of NaCl; sample pH, the pH of water without any adjustment; HCl volume, 10 μL; back-extraction time, 14 min; ultrasounds power, 90%; and ultrasounds frequency, 37 KHz.

3.2. Analytical figures of merit

Quality parameters of the proposed method were evaluated. Under optimized conditions, a concentration range from 0.5 to 25 μg L^{-1} was studied. Finally, the linear working range was established between 0.5 and 10 μg L^{-1}. The calibration curve was constructed using six concentration levels, evaluated by triplicate. The voltammograms corresponding to the blank and the aqueous standards of concentrations from 0.5 to 10 μg L^{-1} are shown in Fig. 3. The resulting calibration curve gave a high level of linearity with a correlation coefficient (r) of 0.997 (N=6). The sensitivity of the instrumental measurements estimated by the slope of the calibration curve was (3.0 ± 0.3) μA μg $^{-1}$ L. The repeatability of the proposed method, expressed as coefficient of variation (CV), was evaluated by five consecutive analyses of aqueous standards at concentrations of 3 and 10 μg L^{-1}. CV values of 13% were found in both cases. An enrichment factor of 25 was obtained for the proposed procedure, defined as the slope ratio of the calibration curves with and without preconcentration.

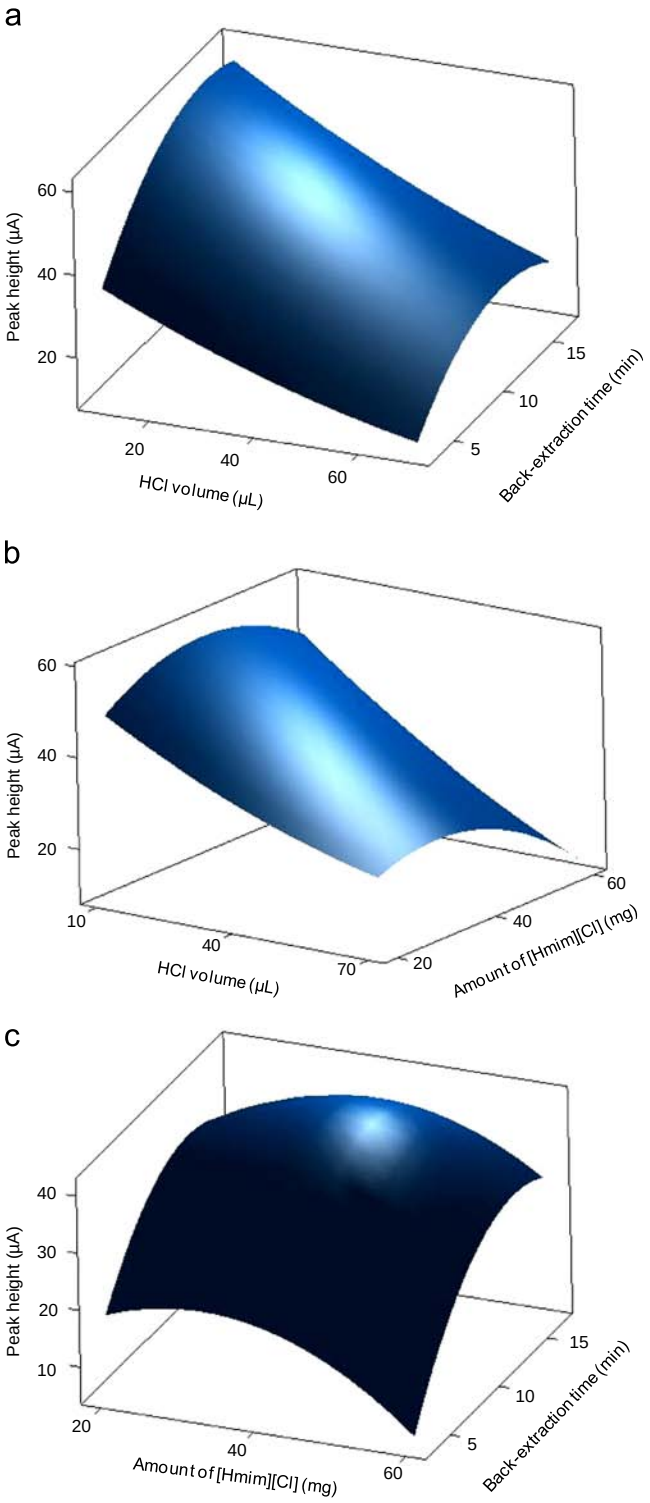

Fig. 2. Surfaces response of CCD design obtained by plotting: (a) HCl volume vs. back-extraction time (amount of [Hmim][Cl]: 40 mg); (b) HCl volume vs. amount of [Hmim][Cl] (back-extraction time: 10 min); and (c) amount of [Hmim][Cl] vs. back-extraction time (HCl volume: 40 μL).

The limit of detection (LOD) was estimated according to the Directive 98/83/EC [5], on the quality of water intended for human consumption, as the concentration corresponding to a signal that is five times the standard deviation of the blank. The LOD was

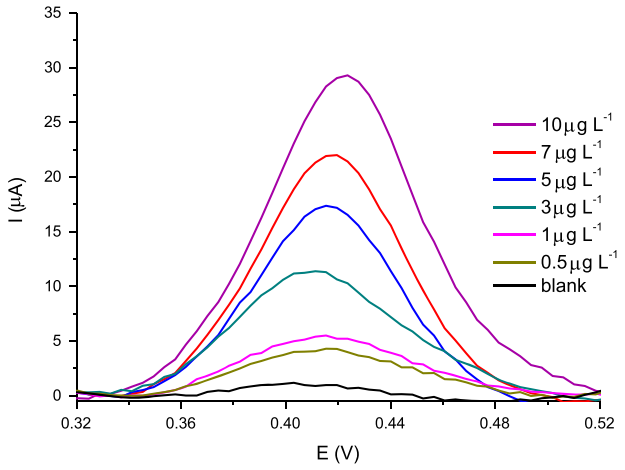

Fig. 3. Square-wave voltammograms, after baseline correction, of a blank and mercury aqueous standards of 0.5, 1, 3, 5, 7 and 10 μg L^{-1} after in-situ IL-DLLME and back-extraction under optimum conditions.

Table 4
Relative recoveries and CV values (in parentheses) for the analysis of mercury in real-world water samples.

Water sample	Relative recoveries	
	1 μg L^{-1}	7 μg L^{-1}
Tap water	106 (11)	108 (7)
Bottled water	98 (11)	103 (15)
River water	97 (10)	98 (9)
Wastewater	97 (12)	95 (9)

found to be 0.2 μg L^{-1}, which is lower than most of the reported works up to now using SPEs (see Table 1), and stands lower than the threshold value established by both, the EPA and the European Union (i.e., 2 μg L^{-1} and 1 μg L^{-1}, respectively). It is important to point out that the sensitivity and LOD of the proposed method are significantly better than those obtained in a previous work [14] (i.e., 0.120 μA μg^{-1} L and 3.3 μg L^{-1}, respectively) using the same kind of SPCnAuEs under equal conditions but without sample preparation. In addition, just a few of the reported works using SPEs have shown equal or lower LOD than 0.2 μg L^{-1} [10,12,14], however, standard addition method was needed to analyze real-world water samples [12,14].

Therefore, the great but scarcely explored advantages that offer the combination of LPME with electrochemical detection using SPEs have been demonstrated.

3.3. Real-world water samples analysis

The applicability of the proposed method to determine mercury in real-world water samples was evaluated studying matrix effects. Four water samples (namely tap water, bottled water, river water and wastewater) were employed for recovery studies. As mentioned before, previous analysis revealed that mercury levels in the samples were under the LOD of the present approach. Three replicated analysis of each water sample were carried out at two different spiking levels (1 and 7 μg L^{-1}). Relative recoveries were calculated as the ratio of the signals found in real and ultrapure water samples spiked at the same concentration level. As can be observed in Table 4, relative recoveries ranged from 95 to 108% in the four water samples, whereas the CV values were between 7 and 15%. According to these results, it can be concluded that the matrix effects were not significant for the determination of mercury in the four selected water samples.

4. Conclusions

SPCnAuEs have been successfully combined with in-situ IL-DLLME and microvolume back-extraction methodologies for the determination of mercury in water samples, reaching a LOD that satisfies the established legal threshold levels and proving its applicability in real-world water sample analysis. Higher sensitivity and lower LOD were obtained with the proposed methodology compared to those obtained with the same electrochemical transducers but omitting the sample preparation. Therefore, the great and up to now practically unexplored benefits that offer the combination of miniaturized sample preparation techniques with the electrochemical analysis using SPEs have been experimentally demonstrated.

Although the ice-bath, centrifugation and sonication limit the in-field application of the proposed methodology, authors strongly believe in a promising future for the synergistic combination of LPME with SPEs as detection methodology within the perspectives of developing inexpensive analytical methodologies with portable options for rapid and on-site measurements.

Acknowledgments

The authors would like to thank the Spanish Ministry of Science and Innovation (Project nos. CTQ2011-23968 and CTQ2011-24560), the Generalitat Valenciana (Spain) (Project nos. ACOMP/2013/072, PROMETEO/2013/038 and GV/2014/096) and the University of Alicante (Spain) (Project no. GRE12-45) for the financial support. E. Fernández and D. Martín-Yerga also thank Generalitat Valenciana and Ministry of Economy and Competitiveness, respectively, for their fellowships.

Appendix A. Supporting information

Supplementary data associated with this article can be found in the online version at http://dx.doi.org/10.1016/j.talanta.2014.11.069.

References

[1] World Health Organization, June 2014, ⟨http://www.who.int/ipcs/assessment/public_health/chemicals_phc/en/index.html⟩.
[2] World Health Organization, June 2014, ⟨http://www.who.int/mediacentre/factsheets/fs361/en/⟩.
[3] K. Leopold, M. Foulkes, P.J. Worsfold, TrAC Trends Anal. Chem. 28 (2009) 426–435.
[4] Environmetal Protection Agency, June 2014, ⟨http://water.epa.gov/drink/contaminants/basicinformation/mercury.cfm⟩.
[5] Council Directive 98/83/EC of 3 November on the quality of water intended for human consumption.
[6] C. Gao, X.-J. Huang, TrAC Trends Anal. Chem. 51 (2013) 1–12.
[7] D. Martín-Yerga, M.B. González-García, A. Costa-García, Talanta 116 (2013) 1091–1104.
[8] E. Bernalte, C. Marín Sánchez, E. Pinilla Gil, Anal. Chim. Acta 689 (2011) 60–64.
[9] F. Arduini, C. Majorani, A. Amine, D. Moscone, G. Palleschi, Electrochim. Acta 56 (2011) 4209–4215.
[10] X. Niu, H. Zhao, M. Lan, Anal. Sci. 27 (2011) 1237–1241.
[11] G. Aragay, J. Pons, A. Merkoçi, J. Mater. Chem. 21 (2011) 4326–4331.
[12] A. Mandil, L. Idrissi, A. Amine, Microchim. Acta 170 (2010) 299–305.
[13] S. Laschi, I. Palchetti, M. Mascini, Sens. Actuators B 114 (2006) 460–465.
[14] D. Martín-Yerga, M.B. González-García, A. Costa-García, Sens. Actuators B 165 (2012) 143–150.
[15] E. Bernalte, C.M. Sánchez, E.P. Gil, Sens. Actuators B 161 (2012) 669–674.
[16] E. Khaled, H.N.A. Hassan, I.H.I. Habib, R. Metelka, Int. J. Electrochem. Sci. 5 (2010) 158–167.
[17] F.W. Campbell, R.G. Compton, Anal. Bioanal. Chem. 396 (2010) 241–259.
[18] F. Pena-Pereira, I. Lavilla, C. Bendicho, TrAC Trends Anal. Chem. 29 (2010) 617–628.
[19] M. Rezaee, Y. Assadi, M.-R. Milani Hosseini, E. Aghaee, F. Ahmadi, S. Berijani, J. Chromatogr. A 1116 (2006) 1–9.
[20] J.M. Kokosa, TrAC Trends Anal. Chem. 43 (2013) 2–13.

[21] H. Yan, H. Wang, J. Chromatogr. A 1295 (2013) 1–15.
[22] M.J. Trujillo-Rodríguez, P. Rocío-Bautista, V. Pino, A.M. Afonso, TrAC Trends Anal. Chem. 51 (2013) 87–106.
[23] M. Baghdadi, F. Shemirani, Anal. Chim. Acta 634 (2009) 186–191.
[24] C. Yao, J.L. Anderson, Anal. Bioanal. Chem. 395 (2009) 1491–1502.
[25] F. Pena-Pereira, I. Lavilla, C. Bendicho, L. Vidal, A. Canals, Talanta 78 (2009) 537–541.
[26] H. Bagheri, M. Naderi, J. Hazard. Mater. 165 (2009) 353–358.
[27] J. Li, W. Lu, J. Ma, L. Chen, Microchim. Acta 175 (2011) 301–308.
[28] X. Jia, Y. Han, X. Liu, T. Duan, H. Chen, Spectrochim. Acta Part B 66 (2011) 88–92.
[29] Z. Gao, X. Ma, Anal. Chim. Acta 702 (2011) 50–55.
[30] E. Stanisz, J. Werner, H. Matusiewicz, Microchem. J. 110 (2013) 28–35.
[31] E. Fernández, L. Vidal, J. Iniesta, J.P. Metters, C.E. Banks, A. Canals, Anal. Bioanal. Chem. 406 (2014) 2197–2204.
[32] G. Martínez-Paredes, M.B. González-García, A. Costa-García, Electrochim. Acta 54 (2009) 4801–4808.
[33] D.C. Montgomery, Design and Analysis of Experiments, seventh ed., Wiley, Hoboken, New Jersey, United States, 2009.
[34] Y.V. Heyden, C. Hartmann, D.L. Massart, L. Michel, P. Kiechle, F. Erni, Anal. Chim. Acta 316 (1995) 15–26.
[35] H. Fabre, N. Mesplet, J. Chromatogr. A 897 (2000) 329–338.
[36] M.D. Priego Capote, F. Luque de Castro, Analytical Applications of Ultrasounds, first ed., Elsevier B.V., Amsterdam, The Netherlands, 2007.